Reliability Evaluation and Improvement of Islanded Microgrid Considering Operation Failures of Power Electronic Equipment

Wen Zhong, Lingfeng Wang, Zhaoxi Liu, and Shiying Hou

***Abstract*—With the high integration of power electronic technologies in microgrids, the reliability assessment considering power electronic devices has become a hot topic. However, so far no research has considered the impact of the operation failure probability of power electronic equipment on the overall reliability of the microgrid. This paper aims to construct a holistic operation failure rate model of power electronic systems based on the overall reliability assessment of islanded microgrid with high penetration of renewable energy sources (RESs). In addition, to improve the reliability of islanded microgrid, the conventional battery energy storage system (BESS) is replaced by the hybrid energy storage system (HESS). Based on the proposed model, the operation failure models for the power electronic modules in microgrid are built and tested, and then the sensitivity analysis is performed for exploring the influence of various factors on the reliability of the microgrid.**

***Index Terms*—Reliability assessment, reliability improvement, operation failure rate, power electronics, islanded microgrid.**

I. Introduction

THE reliability engineering emerged firstly to address the reliability issues in military applications [1]-[3]. There are two methods that are widely adopted. The first one is the empirical reliability model, which is based on the historical operating data [4], [5]. Constant component reliability values are used to evaluate the system reliability indices. This method has been widely applied in the electric power systems to analyze the average reliability indices [6]. However, the empirical approach is independent on the operation condition which means it does not consider the physical cause of electronics' failure. The second one is the physics-based reliability model which was firstly proposed in 1962 [7]-[12]. This method focuses on identifying the root cause mechanism of the component failures and is based on the specific operation condition.

Reference [13] introduces an analytical adequacy assessment method to evaluate the reliability of distribution systems, considering the issues on the renewable distributed generators such as the individual reliability model, protection strategy and islanding operation. However, this method caries out the reliability assessment based on the segments instead of the single individual component. In [14], an evaluation strategy is proposed to investigate the effects of protection schemes on reliability indices for microgrids in different operation conditions. Reference [15] proposes a probabilistic framework to conduct reliability analysis and sizing planning of power systems including the renewable resources and energy storage system (ESS). This method considers the uncertainties of wind turbine generation (WTG), photovoltaic (PV) generation and load shifting strategies to achieve the optimal trade-off between the cost and reliability requirements. Reference [16] presents a reliability assessment method which deploys multi-state models of constituent components (e.g., distributed generation (DG) resources and battery energy storage system (BESS)), and an accelerated Monte Carlo method (MCM) is also proposed and tested. However, this method could cost considerable computational time. In [17], reliability assessment is performed for distribution systems based on sequential MCM, which considers the effects of faults and variations of load demand and generation. Besides, portions of the distribution system can work in islanded mode to supply important loads when there is a fault. Reference [18] proposes a framework to assess the reliability of power distribution system integrated with the mobile BESS (MBESS) and time-varying generation resources. The reliability of the MBESS is analyzed by Markov models, and the distribution system reliability is evaluated by MCM.

High reliability is regarded as one of the main technical

Manuscript received: October 7, 2018; accepted: May 9, 2019. Date of Cross-Check: May 9, 2019. Date of online publication: September 23, 2019.

This work was supported in part by National "111" Project, China (No. B08036), and in part by Chongqing Graduate Student Research Innovation Project, China (No. CYB14015). The first author would like to thank China Scholarship Council for the financial support for her graduate study at the University of Wisconsin-Milwaukee. Also, the authors are grateful to Y. Sang for the initial exploration of this topic.

This article is distributed under the terms of the Creative Commons Attribution 4.0 International License (http://creativecommons.org/licenses/by/4.0/).

W. Zhong is with the State Key Laboratory of Power Transmission Equipment & System Security and New Technology, College of Electrical Engineering, Chongqing University, Chongqing, China, and she is also with Laboratory of Trustworthy Cyber-Physical Systems and Infrastructures, Department of Electrical Engineering and Computer Science, University of Wisconsin-Milwaukee, Milwaukee, USA (e-mail: zw20161102018@163.com)

L. Wang (corresponding author) and Z. Liu are with Laboratory of Trustworthy Cyber-Physical Systems and Infrastructures. Department of Electrical Engineering and Computer Science, University of Wisconsin-Milwaukee, Milwaukee, USA (e-mail: wang289@uwm.edu; zhaoxil@uwm.edu)

S. Hou is with the State Key Laboratory of Power Transmission Equipment & System Security and New Technology, College of Electrical Engineering, Chongqing University, Chongqing, China (e-mail: houshiying@163.com).

DOI: 10.35833/MPCE.2018.000666

advantages of microgrids, and research efforts have been devoted to the reliability analysis of microgrids in recent years [19]-[25]. Most of the existing works explore the reliability by considering the microgrids with the conventional power generations, or together with renewable energy sources (RESs). However, the variable failure and repair rates of the power electronic interfaces are not considered in previous studies. Reference [19] proposes an approach to evaluate the reliability from an operation perspective by matching the generations and loads, in which the components are considered completely reliable. References [20]-[23] focus on the isolated system with constant power output of the generation units, which cannot be applied to the fluctuating renewable generation. Based on variable load profiles, [23] schedules the optimal feeder switching of the system and studies the impact of the transmission system failure on the customer service interruption. To evaluate the reliability more accurately, [24] considers the protection issues to evaluate the reliability indices of the islanded microgrids by using a short-term outage model. Based on this work, [25]-[28] consider the impact of incorrect responses of the protection system and employ the short-term outage model to evaluate the fuzzy reliability indices.

Currently, there are very few works exploring the effects of power electronic devices and meteorological conditions on the overall reliability of islanded microgrids simultaneously. References [26] and [27] introduce the basic reliability indices, reliability assessment methods, and reliability improvement schemes. For the reliability assessment on the component level, the failure rate model proposed in [28] is commonly used in the reliability evaluation of power electronic devices. Based on the above research, [29] proposes a real-time model of multi-level converters in the wind turbine generator.

In addition, to improve the system reliability, several methods focusing on different aspects of the system have been proposed. The first method is to improve the quality of the components; the second method is to refine the thermal management; and the third method is to add redundancy to the system from the hardware and software perspectives. For the redundancy at the system level, it improves the reliability of power electronic systems greatly. However, this method will be highly costly and bring new challenges to the reliability issue of the system. Therefore, the redundancy at the subsystem level is proposed to overcome this disadvantage, improve the reliability of the system greatly with a lower cost and increase the system flexibility [30]. Thus this method is utilized to improve the system reliability in this paper. Simulation results are provided to verify the proposed method in the following section.

While the existing work provides valuable insights on the reliability of microgrids, the variable failure rates of power electronic devices are not considered, which are in fact dependent on a variety of influencing factors. Volatile renewable generations have been widely deployed in microgrids. The failure of power interfaces, which is affected by the operation conditions of the components in the microgrid, would have a negative impact on the overall microgrid reliability. Thus, the operation reliability considering power electronic interfaces has become a critical issue in the reliability study of the microgrid. To deal with this problem, this paper proposes a holistic operation reliability model for the power electronic devices in the microgrid. The failure rates of power electronic devices in the proposed model are calculated according to various operation states. And then the overall microgrid reliability is evaluated quantitatively. Additionally, sensitivity studies are performed to examine the influences of several major factors on the operation reliability of the microgrid .

II. Operational Failure Rate of Power Electronic System

In this section, a comprehensive failure rate model related to power electronics is proposed and illustrated. The model is composed of several procedures which assess the reliability performance of power electronic systems based on the specific operation condition. The proposed model is demonstrated in Fig. 1. The operation condition date are based on the specific operation environment and specific applications. The converter model determines electrical stresses of components. The loss model depends on topology, control, modulation and component parameters. The thermal model determines temperature rise and thermal factors of components. The component reliability model contains empirical and physical models and determines operation failure rate of devices. The system reliability model contains system-level reliability assessment.The input to the general model determines the operation conditions of power electronic systems. Various reliability metrics including the failure rate, reliability and availability can be obtained from the model.

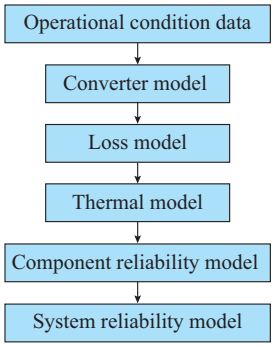

Fig. 1. System-level failure model of reliability assessment procedure.

A. Power Generation Model

1) Output Power of WTG

The power production of WTG systems can be calculated based on the following:

$$P_{WTG}=\begin{cases}P_{wr} & v_r \le v < v_{co} \\ P_{wr}\dfrac{v-v_{ci}}{v_r-v_{ci}} & v_{ci} \le v < v_r \\ 0 & \text{others}\end{cases} \tag{1}$$

where P_{WTG} is the output of the wind turbines; P_{wr} is the rated output of the wind turbines; v is the rated wind speed; v_{ci} is the cut-in wind speed; v_{co} is the cut-out wind speed; and v_r is the rated wind speed [31].

2) Output Power of PV

The power production of the PV system can be calculated by:

$$P_{PV} = P_{sr}\left[1 - 0.0045\left(T_a - E_r\right)\right]\frac{S}{S_r} \tag{2}$$

where P_{PV} is the output of the PV modules; T_a is the ambient temperature; S is the solar illumination; P_{sr} is the rated output of the PV modules; E_r is the reference temperature; and S_r is the reference solar illumination. It can be seen that the output power of PV is primarily determined by the meteorological factors [32].

3) Output Power of Micro-turbine Generator (MTG)

MTGs are considered to be dispatchable generation in the electrical energy systems [33]. MTG is grid-forming DG to support the operation of the system. When it can fully meet the deficiency between the required load and the outputs from other generation subsystems, the output of the micro-turbines can be calculated by:

$$P_{MTG} = P_{RMTG} \tag{3}$$

where P_{MTG} is the output of the MTG; and P_{RMTG} is the rated output of the MTG.

Otherwise, the output of the micro-turbines can be expressed by:

$$P_{MTG} = P_{MTG}^{\max} \tag{4}$$

where $P_{MTG}^{\max}$ is the maximum output of MTG.

4) Power Flow of ESS

In the islanded microgrid deployed with renewable generations, when there is a mismatch between the power supplied by the generation systems and load requirement, the ESS is used to balance the power supply and demand [34]. The ESS acts as a transfer station to store the remaining energy and supply the system when needed. When there is a mismatch between the power supply P_g and load requirements P_{load} and P_{loss}, ESS will fill the gap. To reduce the charging/discharging rate of the ESS, generation system supplies power to the loads with the peer-to-peer control energy management strategy in this paper. Considering the switching losses in the power electronic interfaces in the microgrid, the relationship between the output of different systems in the microgrid can be expressed as:

$$\begin{cases} P_{ESS} + P_g = P_{load} + P_{loss} \\ P_g = P_{WTG} + P_{PV} + P_{MTG} \end{cases} \tag{5}$$

where P_{ESS} is the power flow between the ESS and the microgrid. When the sign of P_{ESS} is positive, it means that ESS is in the discharging mode. Otherwise, ESS is in the charging mode. The worst condition is that when MTG maximizes its output, there is still a mismatch between generation system and load requirements. Thus the micorgrid has to shed some non-priority loads.

B. Power Loss Model

The power loss of voltage source converter (VSC) is the sum of the power losses of the diodes and insulated gate bipolar transistors (IGBTs). The loss of each component (diode or IGBT) can be calculated based on the output power, voltage, current, and switch frequency of the wind turbines, PV modules, ESS or MTGs [32]. The power loss of each diode or IGBT component in the VSC can be expressed as follows [33], [34]:

$$P_{diode} = V_{diode} I\left(\frac{1}{2\pi} \mp \frac{M}{8}\cos\theta\right) + R_{diode} I^2\left(\frac{1}{8} \mp \frac{M}{3\pi}\cos\theta\right) + \frac{f}{\pi}\frac{V_{DC} I}{V_{diode}^{ref} I_{diode}^{ref}} E_{diode} \tag{6}$$

$$P_{IGBT} = V_{IGBT}\left(\frac{1}{2\pi} \pm \frac{M}{8}\cos\theta\right) + R_{IGBT} I^2\left(\frac{1}{8} \pm \frac{M}{3\pi}\cos\theta\right) + \frac{f}{\pi}\frac{V_{DC}}{V_{IGBT}^{ref} I_{IGBT}^{ref}} E_{on} + E_{off} \tag{7}$$

where R_{diode} is the conduction resistance for each diode; E_{diode} is the rated switching loss for each diode; V_{diode} is the voltage drop across the diode; I_{diode}^{ref}, V_{diode}^{ref} are the reference commutation current and voltage, respectively; V_{DC} is DC link voltage; M is the modulation index of different converters; θ is the angle by which the current leads the voltage; I is the peak phase current which can be expressed as (8) [29]; R_{IGBT} is the conduction resistance for each IGBT; V_{IGBT} is the voltage drops across the IGBT; and E_{on}, E_{off} are the power losses of IGBT during the switching operation. For the symbols "$\mp$" in (6) and "$\pm$" in (7), when taking the upper sign, the equation represents the grid-side converter; when taking the lower sign, the calculation is for the power loss of the generator-side converter.

$$I \approx \frac{\sqrt{2}\,P_t}{\sqrt{3}\,U_l} \tag{8}$$

where P_t is the power output of the generation systems or ESSs, and U_l is the line-to-line voltage on the AC side. The total power loss of the converters can be expressed as:

$$P_{loss} = \sum_{i=1}^{N_1} P_{IGBT,i} + \sum_{j=1}^{N_2} P_{diode,j} \tag{9}$$

where N_1 and N_2 are the numbers of IGBTs and diodes in the converters, respectively.

C. Thermal Model

The power losses of the devices can be used as the inputs of the thermal model to obtain the thermal factors of the devices. The thermal model is developed to predict the thermal factors including the junction temperature and temperature variation and detect the thermal cycling of the devices. The junction temperature and temperature variation are critical factors to semiconductor devices [31]. The temperature rise in the converters can be calculated as [29]:

$$T_{module} = T_{ambient} + R_{ha} P_{loss} \tag{10}$$

where $T_{ambient}$ is the ambient temperature; and R_{ha} is the ther-

mal resistance from the ambient to heat sink.

D. Component Reliability Model

In the failure rate model of this study, the hourly failure rates are used. The failure rate model of each component in the system can be expressed as [26]:

$$\lambda_i = \Pi_{PM}\Pi_{process}\Pi_{induced}\left(\gamma_{TH}\Pi_{TH} + \gamma_{TC}\Pi_{TC} + \gamma_M\Pi_M + \gamma_{RH}\Pi_{RH}\right) \tag{11}$$

where Π_{PM} is the manufacturing factor; $\Pi_{process}$ is the aging quality of the component during its lifetime; $\Pi_{induced}$ is the factor of the component's over-stress ability; γ_{TH}, γ_{TC}, γ_M, γ_{RH} are the basic failure rates influenced by temperature, thermal cycling, mechanism and humidity, respectively; λ_i is the failure rate of the i^{th} component in the microgrid; Π_M and Π_{RH} are the mechanical factor and humidity factor, respectively; and Π_{TH}, Π_{TC} are the thermal factor and thermal cycling factors, respectively, and they can be expressed as:

$$\Pi_{TH} = \exp\left(11604 \times 0.44 \times \left(\frac{1}{293} - \frac{1}{T_{ambient} + \Delta T + 273}\right)\right) \tag{12}$$

$$\Pi_{TC} = 12 \times \sqrt[3]{0.5} \times \left(\frac{\Delta T_{cycling}}{20}\right)^{2.5} \exp\left(1414 \times \left(\frac{1}{313} - \frac{1}{T_{\max} + 273}\right)\right) \tag{13}$$

The above equations are for a phase, ΔT = 10 °C, $\Delta T_{cycling}$ is the temperature variation, and $T_{\max}$ is the maximum temperature.

E. System Reliability Model

Building reliability model of subsystems in microgrid is shown in Fig. 2, and the failures caused by thermal overtemperature and thermal cycling can be considered. Because of variations of meteorological factors, output of renewable generation varies from time to time. Thus, the power loss of the power electronics will cause the temperature rise of the components and finally lead to the failure of components.

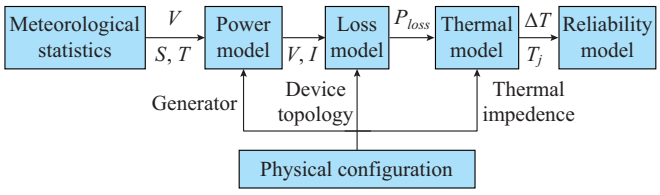

Fig. 2. Operational converter outage model of subsystem.

Based on the above analysis, the reliability metrics of components which contain the failure rate, mean time to failure (MTTF), mean time to repair (MTTR), and availability of the components, can be obtained. Considering each subsystem as a whole, each generation system is in series, thus the failure rate of generation system is the sum of each electronic interface. In addition, hybrid energy storage system (HESS) is a hybrid system, thus the failure rate is evaluated based on the physical configuration and the reliability metrics. At the system level, the fault tree analysis (FTA) method is applied to the reliability evaluation of power electronic systems of the subsystems. Then the obtained reliability metrics are applied to the short-term outage model to evaluate the reliability of the islanded microgrid from the perspectives of customers.

III. Reliability Assessment and Improvement

A. Short-term Outage Model

After obtaining the failure rates of the power electronics from the analysis above, the operation reliability indices considering the time-varying failure rates of the power electronics in the islanded microgrids can be evaluated. The effect of the renewable energy, which contributes to the volatile variation of the temperature of power electronic devices, on the supply of the islanded microgrids can be evaluated through the short-term outage model in this paper. Since the operation failure rate model for each subsystem takes the meteorological and environmental factors into consideration, their failure rates are dependent on time. By utilizing the short-term outage model [24], [25], the operation reliability indices including the outage time and repair rate of each load can be obtained. Based on the operation reliability indices and the power indices from the perspectives of customers analyzed above, the influence of different micro-sources on different loads in the islanded microgrid can be reflected effectively through the time-varying power reliability indices such as system average interruption frequency (SAIFI), system average interruption duration (SAIDI) and energy not supplied (ENS) for the overall islanded microgrids which are shown as follows:

$$\begin{bmatrix} U_1 \\ U_2 \\ \vdots \\ U_N \end{bmatrix} = \begin{bmatrix} r_{11} & r_{12} & \cdots & r_{1M} \\ r_{21} & \gamma_{22} & \cdots & r_{2M} \\ \vdots & \vdots & & \vdots \\ r_{N1} & r_{N1} & \cdots & r_{NM} \end{bmatrix} \begin{bmatrix} \lambda_1 \\ \lambda_2 \\ \vdots \\ \lambda_M \end{bmatrix} \tag{14}$$

$$h(i,j) = \begin{cases} 0 & r_{ij} = 0 \\ 1 & r_{ij} > 0 \end{cases} \tag{15}$$

$$\lambda_{LP,i} = h(i,:)\begin{bmatrix} \lambda_1 \\ \lambda_2 \\ \vdots \\ \lambda_M \end{bmatrix} \quad i = 1, 2, ..., N \tag{16}$$

$$r_{LP,i} = \frac{U_i}{\lambda_{LP,i}} \quad i = 1, 2, ..., N \tag{17}$$

where U_i (i = 1, 2, ..., N) is the outage time of i^{th} load point; matrix $\boldsymbol{r} = (r_{ij})$ represents the repair rate; $h(i,:)$ equals to 1 when its related repair rate has variations, otherwise, it is equal to 0; λ_j (j = 1, 2, ..., M) is the operation failure rate of the j^{th} micro-source system considering the influence of both the operation failure rate of the power electronic system applied in each micro-source generation system and the failure rate of each source; $\lambda_{LP,i}$, $r_{LP,i}$ are the failure rate and repair

time of each load point, respectively. Then the system indices can be expressed as below.

1) SAIFI index (customer per year)

$$S_{AIFI} = \frac{\sum_{i=1}^{N} \lambda_{LP,i} M_i}{\sum_{i=1}^{N} M_i} \tag{18}$$

where M_i is the number of customers in the i^{th} load point.

2) SAIDI index (customer per year)

$$S_{AIDI} = \frac{\sum_{i=1}^{N} U_i M_i}{\sum_{i=1}^{N} M_i} \tag{19}$$

3) ENS index

$$E_{NS} = \frac{\Delta t \sum_{i=1}^{N} L_i}{\sum_{i=1}^{N} M_i} \tag{20}$$

where L_i is the load curtailment; and Δt is the time interval when operation reliability indices are evaluated.

B. Reliability Improvement at Subsystem Level

In the microgrid with high penetration of renewable generation systems, the power fluctuation of storage units includes high-frequency variation due to the uncertainty of meteorological factors and load requirement [27]-[29] and low-frequency variation. Generally, the high-frequency variation requires the energy storage units to respond quickly, which means that they have high power density, while the low-frequency variation requires high energy density of the storage units. Reference [35] proposes a power sharing approach based on the residential load, and it conducts optimal standby assessment of microgrids in both reliable operation and economic aspects through a nonlinear frequency droop scheme.

Batteries are being widely applied as the energy storage equipment in different applications such as hybrid vehicles, utility power systems [36], and DG system. However, it is difficult to recover from fast power fluctuation, and this process will reduce the lifetime of batteries. Nevertheless, none of the single storage unit can provide optimal response to both high-frequency and low-frequency power exchange fluctuations simultaneously [37]. Compared with batteries, energy is stored in or exported from super-capacitors (SCs) by static reaction instead of the electro-chemical reaction in batteries. Thus, the SCs have higher power density and are able to respond faster. From the analysis above, combining different energy storage devices to form HESS can achieve better power and energy performances. This model combines the advantages of each storage device and improves the reliability of the power system. Because the technology of battery and SC is relatively mature, they are being deployed as combined energy storage recently [38], [39]. Reference [40] presents a methodology for optimally sizing RES and ESS in a grid-connected microgrid, considering a number of constraints such as the cost, the reliability, and the effect on environment. In addition, a comparative study is performed to demonstrate that an MG with HESS exhibits a better performance than the battery storage system. Reference [41] presents a comparative study on HESS applied to a power system integrated with RES. Reference [42] proposes a model predictive control scheme for an HESS to decrease the charging rate of batteries and maintain the current and voltage of the ultra-capacitor, thus increasing the lifetime of the battery. The reliability of individual battery modules and power electronic converters is evaluated to perform the reliability assessment of the whole system. A comparative study is carried out for different system configurations and management strategies for BESS. The optimal planning of storage facilities in the distribution system is studied in [43] based on the short-term optimal power flow considering uncertainties. The method aims to minimize the cost by determining the optimal location, capacity and power rating of storage units. Reference [44] proposes a control strategy and a power allocation method for power systems penetrated with WTG and PV generation systems to smooth out the power fluctuation and regulate the state of charge (SOC) of batteries. A new topology is proposed in [45] for HESS applied to electric drive vehicles by replacing the DC/DC converter with smaller capacity, keeping batteries from frequent charging, and increasing the battery life. Reference [46] proposes a systematic method to evaluate the distribution system reliability by considering the effect of telecontrolled distribution switching devices and the islanded operation in distribution system. And this method turns out to be able to enhance the reliability performance.

The commonly used topologies of HESS in microgrid are shown in Fig. 3(a) and (b). As shown in Fig. 3(a), the addition of the SC greatly decreases the electrical stresses of the battery from the perspective of component level. The battery has a relatively low power density. If it is applied in the condition where it is always being charged or discharged suddenly, the failure rate of the battery will increase greatly, and thus decrease the reliability level of the ESS. The topology has a high efficiency.

As shown in Fig. 3(b), SC and batteries are connected in parallel to the microgrid through the DC/AC converter. Each energy storage unit is equipped with the DC/AC converter separately. It can respond fast to the voltage and frequency of the microgrid. Each DC/AC converter can be configured independently to meet its own power demand, but this topology cannot suppress the power fluctuation effectively.

Bidirectional DC/DC converter has the characteristics of low cost and high efficiency. It can realize bidirectional power flow with fewer components and greatly reduce the weight and volume of the system. To realize fast bidirectional power flow of ESS, bidirectional DC/DC converter must be able to switch modes frequently and has two conduction modes: ① complementary PWM conduction mode and ② independent PWM conduction mode [47], [48].

HESS composed of batteries and SCs prolongs the lifetime of batteries and responses faster to intermittent sources. From the perspective of system level, the parallel configuration provides a backup support for ESS. Although HESS is

being widely applied in various applications, the reliability assessment considering the operation failure rate of the power electronics has not been studied yet. To this end, this paper studies the reliability improvement of the islanded microgrids with HESS.

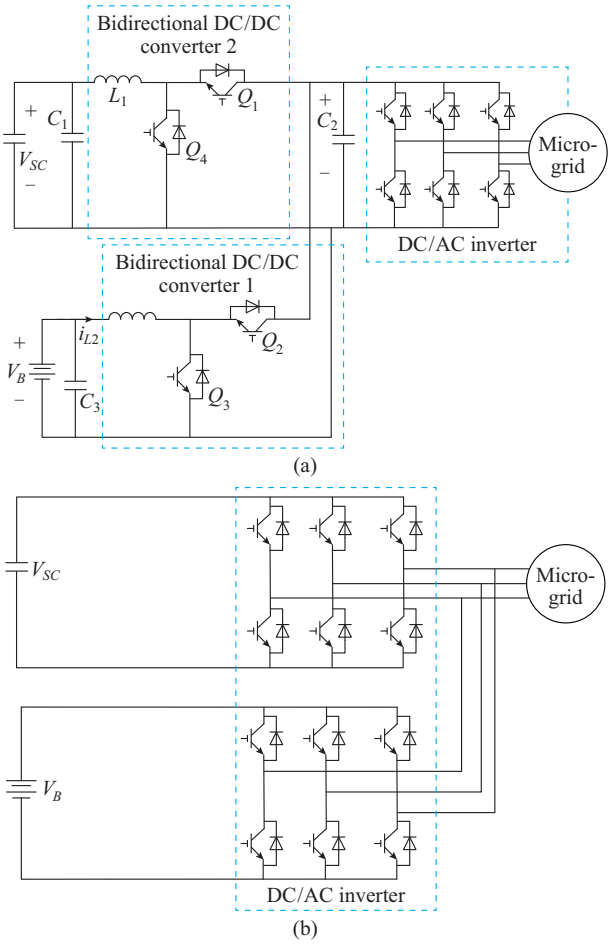

Fig. 3. Topology of HESS islanded microgrid.

IV. Case Studies

A. Test System

A modified benchmark 0.4 kV test system [24] is employed and simulated in the case study. The test system consists of 11 nodes as shown in Fig. 4. The load profile of each load point *LP* and the parameters of the transmission lines *l* are provided in [24]. This tested microgrid system is composed of 12 feeder lines connecting between loads and DGs. In addition, there are tie switches in L6 and L11. When the microgrid works properly, L6 and L11 are open-circuited. The DGs in the system is composed of PVs, WTGs, MTGs and ESS. The PVs and WTGs are considered as uncontrollable micro-sources. There are three PVs, one WTG and one ESS in the system. The rated output and location of DGs are referred in [24], [25] and the main parameters for the power electronic devices in this tested islanded microgrid are referred in [26].

To calculate the systematical reliability indices, the repair rate and failure rate for the modules and breakers are obtained from [24]. In addition, the topologies for the subsystems are illustrated in Fig. 5(a) and (b).

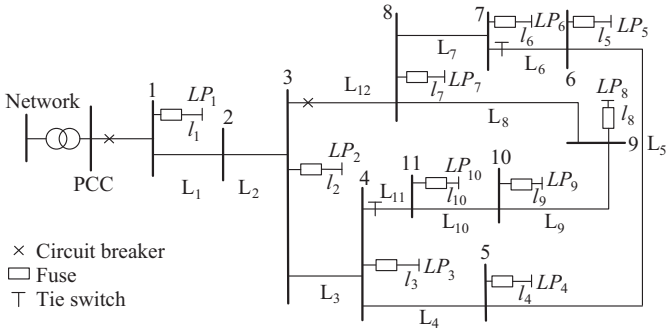

Fig. 4. Modified benchmark 0.4 kV test system.

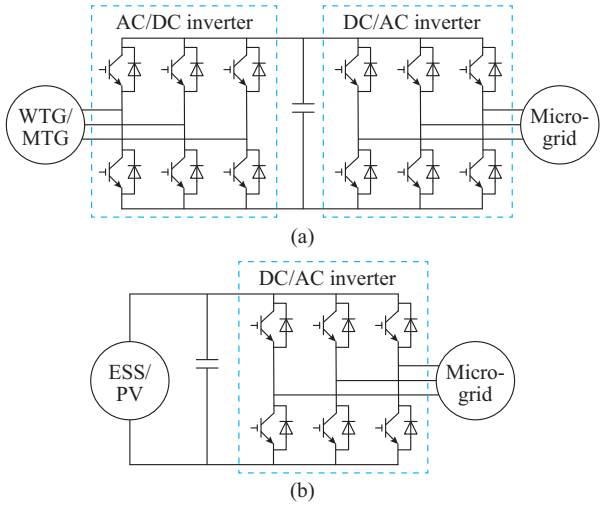

Fig. 5. Topologies for subsystems. (a) A typical grid converter topology of WTGs and MTGs. (b) A typical grid converter topology of PVs and ESS.

B. Meteorological Condition

The meteorological statistics of a given day in summer 2010 in Milwaukee, USA, are shown in Fig. 6.

C. Simulation Results and Analysis

1) Considering Operational Failure Rate of Power Electronics

To verify the proposed model, two cases are studied. In Case 1, the operation failure rates of the power electronics are considered, while they are not considered in Case 2. Both cases use the short-term model to calculate the reliability indices and take the effect of the micro-sources into consideration. The results are shown in Fig. 7.

Comparing the two cases, Case 2 ignores the impact of power electronic failures on the system reliability indices. It only considers the operation condition influence of micro-source fluctuating supply on the reliability indices. As shown in Fig. 7, the reliability indices of Case 1 are all greater than those of Case 2.

Considering the operation impact of the power electronics, the reliability performance of microgrid shows negative trends. In addition, the curves of the three indices are similar to each other. It can be seen that in Case 2, with the empiri-

cal failure rates adopted, it cannot reflect the effect of operation condition on the failure rate of the devices. Since the operation conditions of the microgrids are changeable, the failure rate of the power electronic devices and the parameters such as component failure rate, will directly affect the calculated reliability indices of the load points and the overall system.

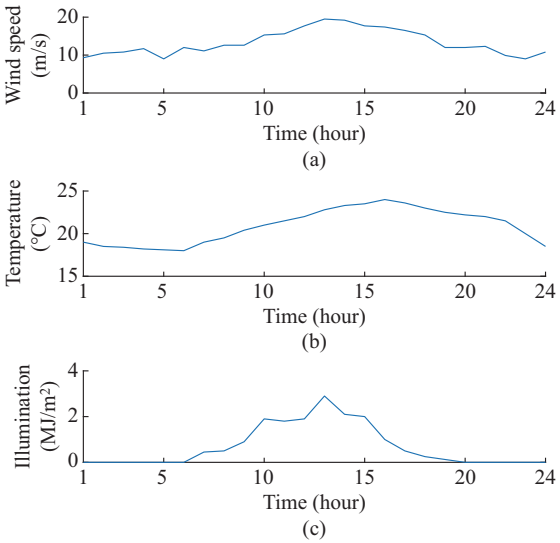

Fig. 6. Meteorological statistics.

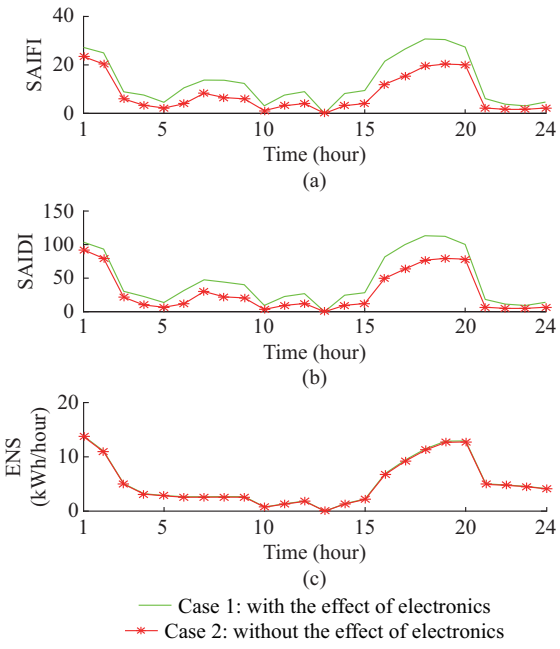

Fig. 7. Reliability indices of Case 1 and Case 2.

2) Validating Proposed Reliability Improvement Method

After building the operation failure model of ESS, to investigate the impact of different types of ESS on the islanded microgrid and verify the effect of the HESS, Cases 1, 3 and 4 are studied. Firstly, BESS without considering bidirectional-DC/DC converter model is built in Case 1. Then, bidirectional-DC/DC converter model is added, and the operation failure model of BESS is built in Case 3. To improve the reliability level of ESS in subsystem level, HESS is applied to the islanded microgrid and the operation failure model of HESS is built in Case 4. The hourly reliability indices of these cases are calculated and illustrated in Fig. 8.

The results are shown in Fig. 8. By comparing Case 3 and Case 4, the reliability indices decrease obviously, which indicates that the microgrid with HESS shows a better performance than the microgrid with BESS. This approach adds a redundant support for ESS. When the batteries or SCs have failure, ESS can still partly maintain its performance to supply the customers. Thus, the comparison of the two cases verifies the reliability improvement method presented in Section III.

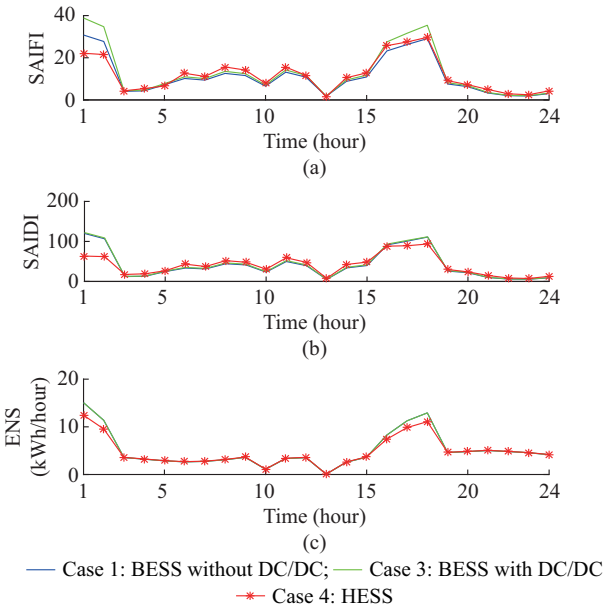

Fig. 8. Reliability indices of Cases 1, 3, and 4.

Comparing Case 1 and Case 3, the addition of bidirectional DC/DC converter increases the operation failure rate of ESS, because the failure rates of batteries are assumed to have the same value in these two cases. In practice, the bidirectional DC/DC converter will decrease the electrical stresses and amount of the batteries, and thus the failure rate of the batteries will be smaller. Therefore, finding a balance between the added redundancy to the system and the increase of failure rate caused by power electronics is of great significance. It can be seen from the results that the large-scale application of power electronic devices also brings new hidden danger for the reliability of microgrid systems. Improving the reliability of high-power converter circuits is an urgently needed part of microgrid technology.

3) Considering Different Types of Micro-sources

This part explains the different types of micro-source impact on the reliability performance of the islanded microgrid. PV and WTG systems are uncontrollable generations and the MTG system falls into controllable generations.

For the 1st condition, the islanded microgrid is fully supplied by renewable energy generation systems (WTG and PV). Four cases as listed in Table I are analyzed, and the re-

liability indices for the overall system are calculated.

TABLE I
FOUR CASES UNDER 1ST CONDITION

Case	Condition
1	1 WTG + 3 PVs
5	4 PVs
6	2 PVs + 2 WTGs
7	4 WTGs

Figure 9 shows that as compared with Case 1, the reliability indices of Case 5 including SAIDI and SAIFI decrease while ENS increases. Compared with Case 1, the PV system shows better performance because the operation failure rate of the PV system (one stage) is smaller than the WTG system (two stages). However, when the system is fully powered by all WTG systems in Case 7, the system reliability decreases greatly since all the reliability indices including SAIDI, SAIFI and ENS increase. Because of the highly integrated power electronics, the negative impact of power electronic failures on reliability indices is significant. In addition, it can be found that when the PV system is replaced by the WTG system, the overall reliability indices show an upward trend.

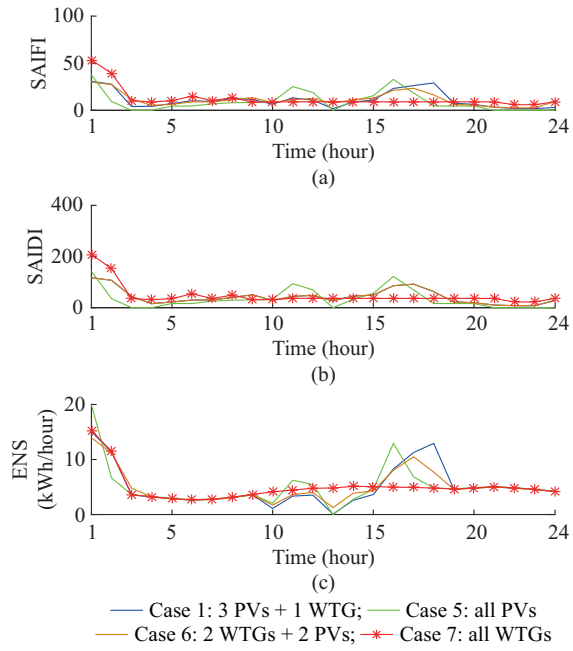

Fig. 9. Reliability indices of Cases 1, 5, 6, and 7.

For the 2nd condition, three cases as listed in Table II are analyzed to compare the reliability performance of microgrid with controllable generation system by replacing the WTG or PV system with the MTG system. The comparison and figures of the reliability indices are illustrated below.

As shown in Fig. 10, the microgrid in Case 8 shows better performance compared to Case 1. All the three indices decrease greatly, especially ENS. Because the MTG system has the same topology as the WTG system, the effect of operation failure rate is similar. In addition, the power output of MTG can be controlled based on load requirements. Based on Case 8, when replacing one PV system with WTG, the resulting indices SAIDI and SAIFI of Case 9 increase because the impact of electronic devices is greater. However, ENS decreases because WTG shows better performance in power supply.

TABLE II
THREE CASES UNDER 2ND CONDITIONS

Case	Condition
8	1 MTG + 3 PVs
9	1 MTG + 2 PVs + 1 WTG
10	1 MTG + 3 WTGs

Based on Case 8, all the PV systems are replaced with WTG systems in Case 10. As analyzed above, the microgrid has better performance, and all the reliability indices decrease. From the analysis above, it is shown that the types of micro-sources have great influence on reliability indices of the overall system.

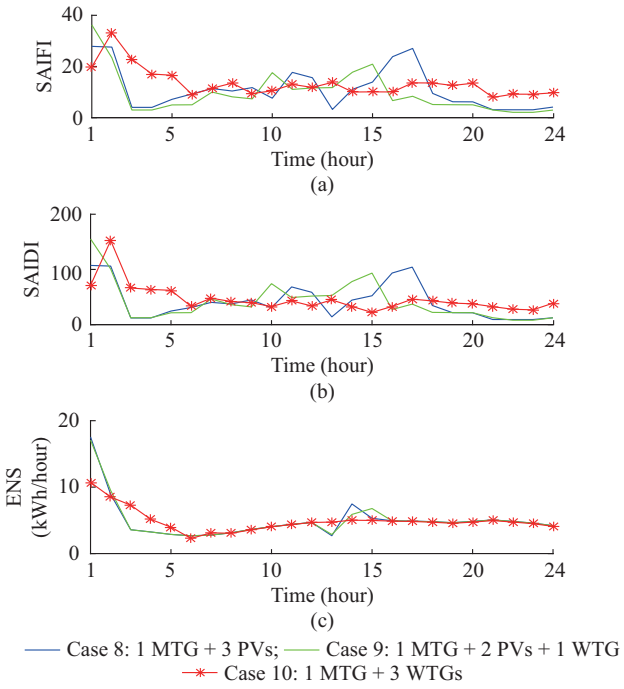

Fig. 10. Reliability indices of three cases.

V. SENSITIVITY STUDIES

A. Effect of Wind Turbine Parameter

The parameters of wind turbines can affect the output power of WTG and consequently affect the reliability metrics of the components. Thus, they have the influence on the failure rate of the system.

1) Cut-in Wind Speed

In this section, the effect of v_{ci} on the system reliability performance is further studied. v_{ci} is set with different values from 2.5 m/s to 4.0 m/s in the test. The setting values are all

less than v_r , and the hourly operation failure rates of WTG are shown in Fig. 11.

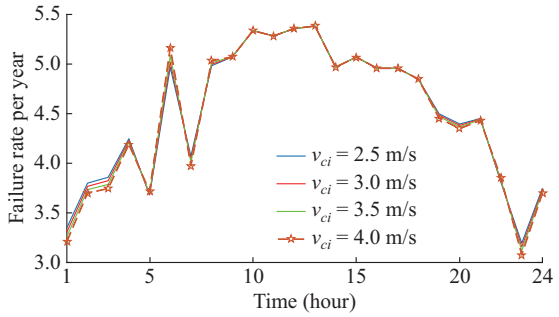

Fig. 11. Hourly operation failure rate of WTGs considering cut-in wind speed.

From the power model of WTG, it is obvious that when v_{ci} increases, the generation of WTGs decreases. Figure 11 shows that with the increase of cut-in speed, the power generation ability is weakened. It means that the power generated decreases and the electrical stresses of power electronics decrease accordingly.

2) Cut-out wind speed

To further study the impact of v_{co} on the reliability performance, v_{co} is set as different values from 14 m/s to 20 m/s. The setting values are all greater than V_r, and the hourly operation failure rates of WTGs are shown in Fig. 12. It is obvious that, the generation of the wind turbine generators increases when v_{co} is increased.

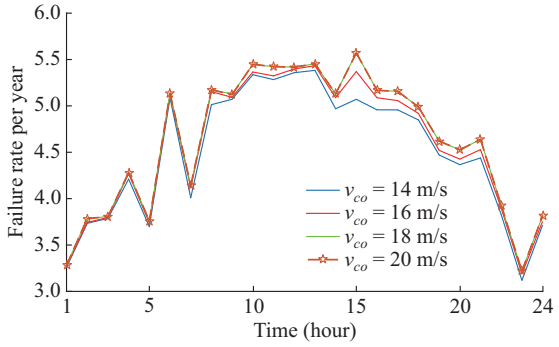

Fig. 12. Hourly operation failure rates of WTGs considering cut-out wind speed.

As shown in Fig. 12, v_{co} has slight effect on the operation failure rate of the converter. When v_{co} increases, the power generation capability is improved at the first change of the parameter, then stays as the same. It is because the power supply increases and the electrical stress increases, thus the failure rate is slightly greater.

3) Rated Wind Speed

To further study the impact of v_r on reliability performance, v_r is set as different values from 11.5 m/s to 14.5 m/s in the test. The setting values are all in the range between v_{ci} and v_{co}. The operation failure rates of the WTG system in different conditions are shown in Fig. 13.

As shown in Fig. 13, v_r has great effect on the operation failure rate of the converter, especially from hour 1 to hour 11. With v_r increases, the power generation decreases, which means that the electrical stresses decrease, thus the failure rate is lower .

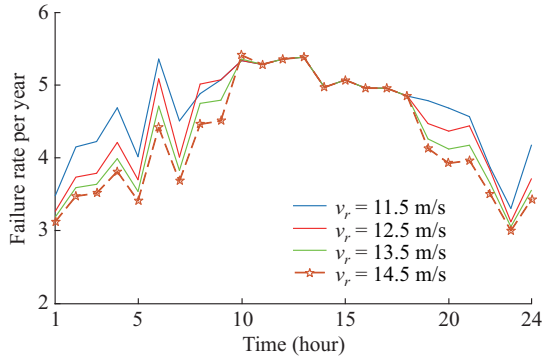

Fig. 13. Hourly operation failure rates of WTGs considering rated wind speed.

B. Effect of PV Parameters

For the PV arrays, the parameters including E_r, S_r and G_r (rated generation) will also affect the output of PV generation and the operation condition of converters, and consequently have influence on the failure rates of the overall system.

1) Rated solar illumination

In this section, the effect of S_r on the reliability performance is further studied. The rated solar illumination is set as different values. The hourly operation failure rates of PV system are shown in Fig. 14. When the rated solar illumination increases, the generation of PV arrays decreases.

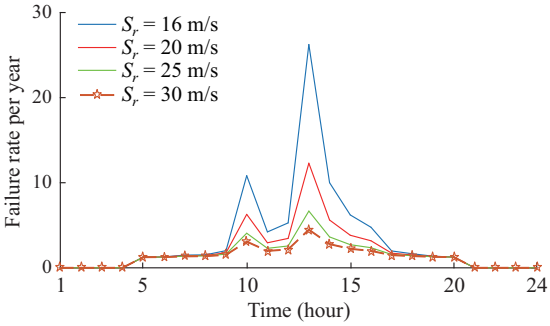

Fig. 14. Hourly operation failure rates of PV system with rated solar illumination.

From the power model of PV, it is obvious that when the rated solar illumination increases, the output of the PV arrays decreases greatly. As shown in Fig. 14, with the increased rated solar illumination, the power generation ability is weakened, which means the power generated decreases and the electrical stresses of power electronics decrease accordingly, thus the operation failure rate of PV system decreases.

2) Rated Temperature

To further study the impact of E_r on the reliability performance, the rated temperatures of PV arrays are set as 16, 20, 25 and 30 centigrade, respectively. The hourly operation failure rates of PV system are shown in Fig. 15.

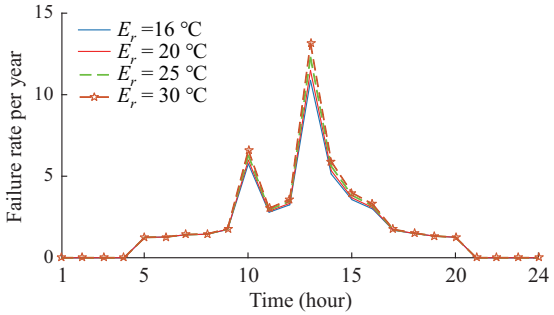

Fig. 15. Hourly operation failure rates of PV system with rated temperature.

As shown in Fig. 15, the rated temperature has great effect on the operation failure rate of the converter. When this parameter increases, the output of PV arrays increases. The effect is more obvious from hour 12 to hour 14, because the solar illumination is stronger during this period and thus the output of PV arrays increases greatly. In contrast, the effect is slight from 0 to hour 9. As the solar illumination gets stronger, the power generation ability of the PV arrays increases. The electrical stresses increase, and consequently, the failure rate is higher.

3) Rated Generation

To further study the impact of the rated generation on the reliability performance, the rated generation of PV arrays is set as different values. The hourly operation failure rates of PV are shown in Fig. 16.

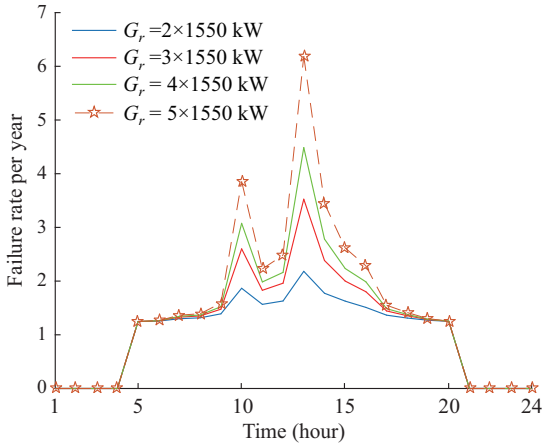

Fig. 16. Hourly operation failure rate of PV system with rated generation.

From the power model of PV, it is obvious that when the rated generation increases, the generation of PV arrays increases. As shown in Fig. 16, the gap between the curves is bigger from hour 12 to hour 14. Because during this period, the solar illumination is stronger and reaches the peak at hour 13, and thus the output of PV arrays increases greatly. When the output of PV arrays increases, the electrical stresses of the devices are heavier, and consequently the failure rate increases when the rated generation increases.

C. Effect of ESS Capacity

For the islanded microgrid with high penetration of RES, ESS plays an important role in mitigating the uncertain characteristics of the renewable power. To verify the effect of the ESS capacity on system reliability, the capacity of the battery in ESS is adjusted from 500 kW and 1250 kW in the test. As shown in the test results, the reliability indices increase with the growth of battery capacity.

When the capacity of ESS increases, the power flow through power electronics in ESS gets higher, and thus the electrical stresses of the devices increase. In general, the failure rate increases when battery capacity increases. In addition, the reliability indices of the microgrid are shown in Fig. 17.

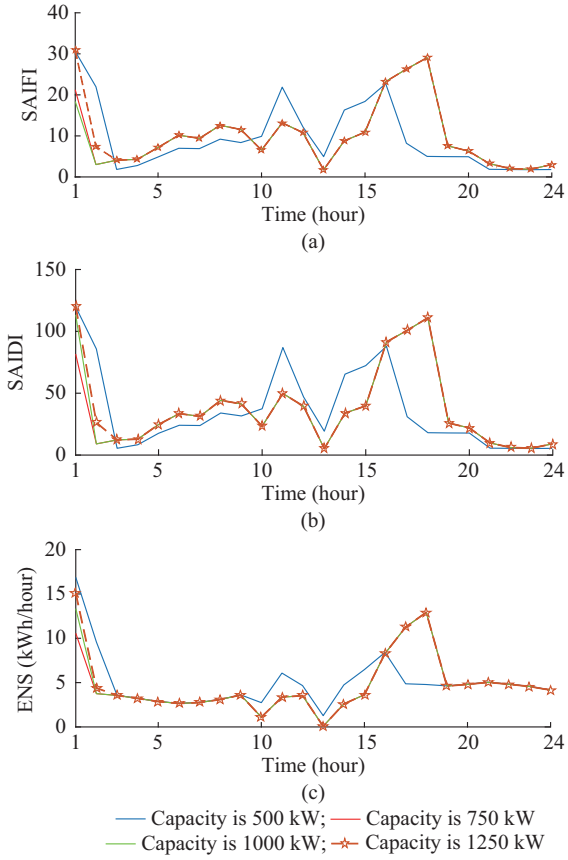

Fig. 17. Hourly reliability indices for different capacities.

As the results shown above, when the capacity of ESS increases, the electrical stresses of power electronics in conversion system increase, and therefore the failure rate of this subsystem increases. Thus, the values of SAIDI and SAIFI increase while ENS decreases in general. As shown in the figures above, the reliability indices with larger ESS capacity are higher than the cases with smaller ESS capacity from hour 17 to hour 18. It is because during the time, the load of the microgrid is heavy, the power flow of ESS is high, and therefore the probability of load outage and ENS is higher.

D. Characteristics of Yearly Operational Failure Rate

For the study of yearly operation failure rate of islanded

microgrid in this paper, the meteorological statistics in the whole year 2010 in Milwaukee are used and shown in Figs. 18-20.

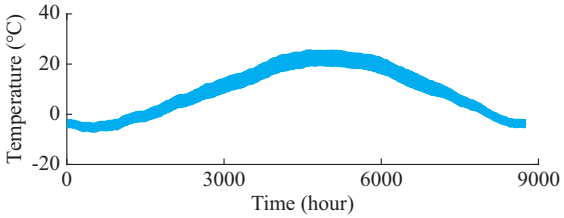

Fig. 18. Ambient temperature in Milwaukee, 2010.

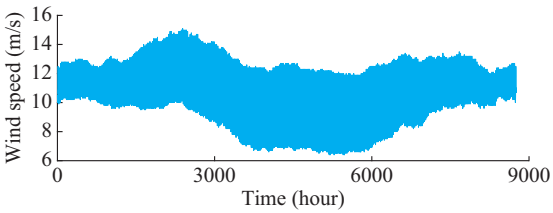

Fig. 19. Wind speed in Milwaukee, 2010.

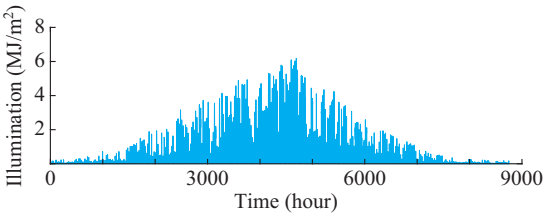

Fig. 20. Solar illumination in Milwaukee, 2010.

Based on the statistics in the figures above, the WTG and the operation failure rates for the power electronics are calculated and shown in Figs. 21-22.

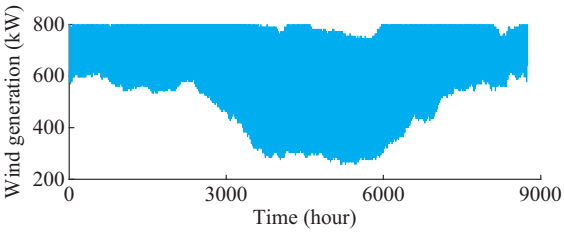

Fig. 21. Hourly wind generation.

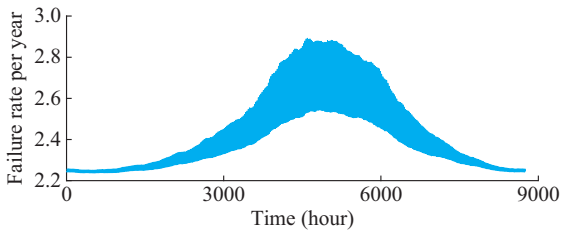

Fig. 22. Hourly failure rates of power electronics in WTG system.

As shown in the figures above, the wind generation reflects the wind speed fluctuation in summer and autumn directly, and the trend of the hourly generation curve is consistent with the wind speed. The relatively lower failure rate for the WTG system appears from 0 to hour 2000 and from hour 7000 to hour 8760. Because the meteorological factors such as lower wind speed and lower temperature cause less power generation, the thermal factor of power electronics are smaller, and the failure rate during the period is smaller. The operation failure rate shows a closer relationship with the ambient temperature, and it also reflects seasonal fluctuation of wind power.

Based on meteorological statistics, the hourly solar generation and operation failure rate for PV are calculated and shown in Figs. 23 and 24.

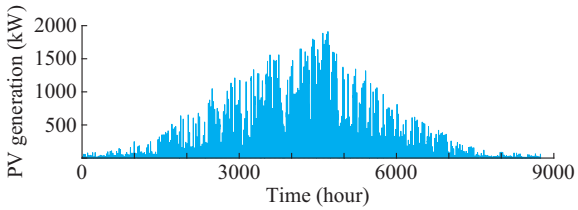

Fig. 23. Hourly solar generation.

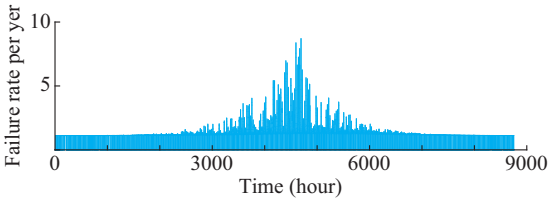

Fig. 24. Hourly failure rate of power electronics in PV system.

As shown in the above figures, from hour 2000 to hour 4800, the solar generation reflects the hourly solar illumination in general. For the operation failure rate of PV systems, it shows an upward trend and reaches the highest point around hour 4800 because of the strong solar illumination and high temperature around that time. Then, it starts to decrease but still remains on a high level from hour 4800 to hour 6200. The trend of the hourly converter failure rate curve is consistent with the ambient temperature, and it also reflects the fluctuation of solar illumination in summer and autumn.

VI. Conclusion

Large-scale application of power electronic devices greatly impacts the reliability of microgrids. The operation reliability indices for a modified 0.4 kV islanded benchmark system are evaluated and the proposed operation model is verified in this paper. To improve the system reliability, the conventional BESS are replaced with HESS. The results show that the system reliability with HESS has a better performance than the system with BESS. Finally, the sensitivity analysis is performed to study the influence of several relevant factors on the system reliability.

Based on the work in this paper, additional research efforts can be focused on the following aspects.

1) Considering more weather conditions such as extreme weather conditions in component failure model and studying

their impact on system reliability.

2) Integrating forecasting technology for meteoro-logical factors to predict the system failure rate prediction.

3) Calculating the unavailability of each subsystem and analyzing the contribution of each component to system reliability.

4) Performing economic analysis. Finding the optimal trade-off between the reliability and cost considering the investment and the maintenance to choose the optimal topology of HESS.

5) Calculating the system reliability for multiple systems with different topology, considering the connection to the distribution network and calculating more reliability indices with the load.

6) Analyzing more parameters for generation system and ESS for the sensitivity part.

REFERENCES

[1] W. Denson, "The history of reliability prediction," *IEEE Transactions on Reliability*, vol. 47, no. 3, pp. 321-328, 1998.

[2] R. Billinton and R. N. Allan, *Reliability evaluation of power systems*, 2nd ed. New York, USA: Plenum Press, 1996.

[3] M. G. Pecht and F. R. Nash, "Predicting the reliability of electronic equipment," *Proceedings of the IEEE*, vol. 82, no. 7, pp. 992-1004, Jul. 1994.

[4] Reliability prediction of electronic equipment: military handbook, Department of Defense, Washington, USA, 1986.

[5] M. Rausand, "System reliability theory: models, statistical methods, and applications," in *Statistical methods in reliability theory and practice*, 2nd ed. England, UK: E. Horwood, 2004.

[6] K. Chatterjee, K. Modarres, and J. B. Bernstein "Fifty years of physics of failure," *Journal of the Reliability Information Centerel*, vol. 20, no. 1, pp. 1-5, Jan. 2012.

[7] A. Dasgupta, K. Sinha, and J. Herzberger, "Reliability engineering for driver electronics in solid-state lighting products," in *Solid State Lighting Reliability*, New York, USA: Springer, 2013, pp. 243-284.

[8] J. G. Mcleish, "Enhancing MIL-HDBK-217 reliability predictions with physics of failure methods," in *Proceedings of 2010 Annual Reliability and Maintainability Symposium*, San Jose, USA, Jan. 2010, pp. 1-6.

[9] H. Wang, M. Liserre, F. Blaabjerg *et al*., "Transitioning to physics-of-failure as a reliability driver in power electronics," *IEEE Journal of Emerging and Selected Topics in Power Electronics*, vol. 2, no. 1, pp. 97-114, Mar. 2014.

[10] M. Pechtand and A. Dasgupta, "Physics-of-failure: an approach to reliable product development," in *Proceedings of IEEE International Integrated Reliability Workshop*, Lake Tahoe, USA, Oct. 1995.

[11] K. Ma, Y. Yang, and F. Blaabjerg, "Transient modelling of loss and thermal dynamics in power semiconductor devices," in *Proceedings of IEEE Energy Conversion Congress and Exposition*, Pittsburgh, USA, Sept. 2014.

[12] I. S. Bae and J. O. Kim, "Reliability evaluation of customers in a microgrid," *IEEE Transactions on Power Systems,* vol. 23, no. 3, pp. 1416-1422, Sept. 2008.

[13] C. Chen, W. Wu, B. Zhang *et al*., "An analytical adequacy evaluation method for distribution networks considering protection strategies and distributed generators," *IEEE Transactions on Power Delivery*, vol. 30, no. 3, pp. 1392-1400, May 2015.

[14] X. Xu, T. Wang, L. Mu *et al*., "Predictive analysis of microgrid reliability using a probabilistic model of protection system operation," *IEEE Transactions on Power Systems*, vol. 32, no. 4, pp. 3176-3184, Nov. 2017.

[15] A. Arabali, M. Ghofrani, M. Etezadiamoli *et al*., "Stochastic performance assessment and sizing for a hybrid power system of solar/wind/energy storage," *IEEE Transactions on Sustainable Energy*, vol. 5, no. 2, pp. 363-371, Apr. 2014.

[16] T. Yan, W. Tang, Y. Wang *et al*., "Reliability assessment of a multi-state distribution system with microgrids based on an accelerated Monte-Carlo method," *IET Generation, Transmission & Distribution*, vol. 12, no. 13, pp. 3221-3229, Jul. 2018.

[17] M. D. Q. Pilar, J. Contreras, A. Mazza *et al*., "Reliability assessment of microgrids with local and mobile generation, time-dependent profiles, and intra-day reconfiguration," *IEEE Transactions on Industry Applications*, vol. 54, no. 1, pp. 61-72, Jan.-Feb. 2018.

[18] Y. Chen, Y. Zheng, F. Luo *et al*., "Reliability evaluation of distribution systems with mobile energy storage systems," *IET Renewable Power Generation*, vol. 10, no. 10, pp. 1562-1569, Nov. 2017.

[19] S. B. Patra, J. Mitra, and S. J. S. Ranade, "Microgrid architecture: a reliability constrained approach," in *Proceedings of IEEE PES General Meeting*, San Francisco, USA, Jun. 2005, pp. 2372-2377.

[20] J. Mitra, S. B. Patra and S. J. Ranade, "Reliability stipulated microgrid architecture using particle swarm optimization," in *Proceedings of 2006 International Conference on Probabilistic Methods Applied to Power Systems*, Stockholm, Sweden, Jun. 2006, pp. 1-7.

[21] A. K. Basu, S. Chowdhury, D. Ray *et al*., "Reliability study of a micro-grid power system," in *Proceedings of 2008 43rd International Universities Power Engineering Conference*, Padova, Italy, Sept. 2008, pp. 1-4.

[22] A. Prasai, A. Paquette, Y. Du *et al*., "Minimizing emissions in microgrids while meeting reliability and power quality objectives," in *Proceedings of 2010 International Power Electronics Conference* (*ECCE ASIA*), Sapporo, Japan, Jun. 2010, pp. 726-733.

[23] S. Yin and C. Lu, "Distribution feeder scheduling considering variable load profile and outage costs," *IEEE Transactions on Power Systems*, vol. 24, no. 2, pp. 652-660, Mar. 2009.

[24] X. Xu, J. Mitra, T. Wang *et al*., "Evaluation of operational reliability of a microgrid using a short-term outage model," *IEEE Transactions on Power Systems*, vol. 29, no. 5, pp. 2238-2247, Feb. 2014.

[25] X. Xu, J. Mitra, T. Wang *et al*., "An evaluation strategy for microgrid reliability considering the effects of protection system," *IEEE Transactions on Power Delivery*, vol. 31, no. 5, pp. 1989-1997, Aug. 2016.

[26] R. Karki, R. Billinton and A. K. Verma, "Reliability modeling and analysis of smart power systems," New Delhi, India: Springer, 2014.

[27] Y. Song and B. Wang, "Survey on reliability of power electronic systems," *IEEE Transactions on Power Electronics*, vol. 28, no. 1, pp. 591-604, Apr. 2013.

[28] FIODES Guide 2009 Edition, A Reliability Methodology for Electronic Systems, 2009.

[29] K. Xie, Z. Jiang, and W. Li, "Effect of wind speed on wind turbine power converter reliability," *IEEE Transactions on Energy Conversion*, vol. 27, no. 1, pp. 96-104, Mar. 2012.

[30] M. K. Rahmat and S. Jovanovic, "Reliability modelling of uninterruptible power supply systems using fault tree analysis method," *European Transactions on Electrical Power*, vol. 19, no. 2, pp. 258-273, Mar. 2009.

[31] B. Hayes, "Reliability assessment of active distribution networks considering distributed energy resources and operational limits," in *Proceedings of CIRED Workshop 2016*, Helsinki, Finland, Jun. 2016, pp. 1-4.

[32] W. G. Scott, "Micro-turbine generators for distribution systems," *IEEE Industry Applications Magazine*, vol. 4, no. 3, pp. 57-62, 1998.

[33] H. Zhang and L. M. Tolbert, "Efficiency impact of silicon carbide power electronics for modern wind turbine full scale frequency converter," *IEEE Transactions on Industrial Electronics*, vol. 58, no. 1, pp. 21-28, Jan. 2011.

[34] H. Wang, M. Liserre, F. Blaabjerg *et al*., "Transitioning to physics-of-failure as a reliability driver in power electronics," *IEEE Journal of Emerging & Selected Topics in Power Electronics*, vol. 2, no. 1, pp. 97-114, Mar. 2014.

[35] F. Cingoz, A. Elrayyah, and Y. Sozer, "Optimized resource management for PV-fuel cell based microgrids using load characterizations," *IEEE Transactions on Industry Applications*, vol. 52, no. 2, pp. 1723-1735, Mar.-Apr. 2016.

[36] N. Mendis, K. M. Muttaqi, and S. Perera, "Management of battery-supercapacitor hybrid energy storage and synchronous condenser for isolated operation of PMSG based variable-speed wind turbine generating systems," *IEEE Transactions on Smart Grid*, vol. 5, no. 2, pp. 944-953, Mar. 2014.

[37] X. Tan, Q. Li, and H. Wang, "Advances and trends of energy storage technology in microgrid," *International Journal of Electrical Power & Energy Systems*, vol. 44, no. 1, pp. 179-191, Jan. 2013.

[38] H. Chen, T. Cong, W. Yang *et al*., "Progress in electrical energy storage system: a critical review," *Progress in Natural Science: Materials International*, vol. 19, no. 3, pp. 291-312, Jan. 2009.

[39] H. Wang, X. Yang, and M. Zhang, "A control strategy of hybrid energy storage system capable of suppressing output of photovoltaic generation system," *Power System Technology*, vol. 37, no. 9, pp. 2542-2548, Dec. 2013.

[40] U. Akram, M. Khalid, and S. Shafiq, "An innovative hybrid wind-so-

lar and battery-supercapacitor microgrid system—development and optimization," *IEEE Access*, vol. 5, pp. 25897-25912, Oct. 2017.
[41] A. Mamen and U. Supatti, "A survey of hybrid energy storage systems applied for intermittent renewable energy systems," in *Proceedings of IEEE 14th International Conference on Electrical Engineering/ Electronics, Computer, Telecommunications and Information Technology (ECTICON)*, Phuket, Thailand, Jun. 2017, pp. 729-732.
[42] B. Hredzak, V. G. Agelidis, and M. Jang, "A model predictive control system for a hybrid battery-ultracapacitor power source," *IEEE Transactions on Power Electronics*, vol. 29, no. 3, pp. 1469-1479, Jun. 2014.
[43] M. Liu, W. Li, C. Wang *et al*., "Reliability evaluation of large scale battery energy storage systems," *IEEE Transactions on Smart Grid*, vol. 8, no. 6, pp. 2733-2743, Mar. 2017.
[44] X. Li, D. Hui, and X. Lai, "Battery energy storage station (BESS)-based smoothing control of photovoltaic (PV) and wind power generation fluctuations," *IEEE Transactions on Sustainable Energy*, vol. 4, no. 2, pp. 464-473, Apr. 2013.
[45] J. Cao and A. Emadi, "A new battery/ultracapacitor hybrid energy storage system for electric, hybrid, and plug-in hybrid electric vehicles," *IEEE Transactions on Power Electronics*, vol. 27, no. 1, pp. 122-132, Feb. 2012.
[46] S. Conti, S. A. Rizzo, E. F. El-Saadany *et al*., "Reliability assessment of distribution systems considering telecontrolled switches and microgrids," *IEEE Transactions on Power Systems*, vol. 29, no. 2, pp. 598-607, Mar. 2014.
[47] Z. Lu, W. Zhu, J. Liu *et al*., "A novel interleaved parallel bidirectional DC/DC converter," in *Proceedings of the Chinese Society of Electrical Engineering*, vol. 33, no. 12, pp. 39-46, Apr. 2013.
[48] G. Zhang, X. Tang, L. Zhou *et al*., "Research on complementary PWM controlled buck/boost bi-directional converter in supercapacitor energy storage," *Proceedings of the CSEE*, vol. 31, no. 6, pp. 15-21, Feb. 2011.

Wen Zhong received the B.S. degree in electrical engineering from Hubei University of Technology, Wuhan, China, in 2016 and the M.S degree of University of Wisconsin – Milwaukee (UWM), Milwaukee, USA, in 2018. She is currently pursuing the M. S degree in electrical engineering of Chongqing University, Chongqing, China. Her research interests include microgrids, power system analysis, power system reliability assessment, and control strategy of hybrid energy storage system.

Lingfeng Wang is currently a Professor with the Department of Electrical Engineering and Computer Science, University of Wisconsin – Milwaukee, Milwaukee, USA, where he directs the cyber-physical energy systems research group. He was an Assistant Professor with the University of Toledo, Toledo, USA, and an Associate Transmission Planner with the California Independent System Operator, Folsom, USA. His current research interests include power system reliability and resiliency, smart grid cybersecurity, critical infrastructure protection, energy-water nexus, renewable energy integration, intelligent and energy-efficient buildings, electric vehicles integration, microgrid analysis and management, and cyber-physical systems.

Zhaoxi Liu received the B.S. and M.S. degrees in electrical engineering from Tsinghua University, Beijing, China, in 2006 and 2008, respectively. He obtained the Ph.D. degree in electrical engineering from Technical University of Denmark, Copenhagen, Denmark, in 2016. He is currently a research associate in the Department of Electrical Engineering and Computer Science, University of Wisconsin – Milwaukee, Milwaukee, USA. His research interests include power system cybersecurity and resiliency, power system operations, and integration of distributed energy resources in power systems.

Shiying Hou received the B.S., M.S., and Ph.D. degrees from the Department of Electrical Engineering, Chongqing University, Chongqing, China, in 1982, 1999, and 2008, respectively. She is currently a Professor in the Department of Electrical Engineering, Chongqing University. Her research interests include control theory and its applications, power electronic technology in power systems, and renewable energy grid integration.